Supporting Information

Core-shell CuPd@Pd tetrahedra with concave structure and Pd-enriched surface boost formic acid oxidation

Yifan Chen,[a] Yifan Yang,[a] Gengtao Fu,*[b] Lin Xu,[a] Dongmei Sun,[a] Jong-Min Lee,*[b] and Yawen Tang*[a]

[a] Jiangsu Key Laboratory of New Power Batteries, Jiangsu Collaborative Innovation Centre of Biomedical Functional Materials, School of Chemistry and Materials Science, Nanjing Normal University, Nanjing 210023, China.

[b] School of Chemical and Biomedical Engineering, Nanyang Technological University, Singapore 637459, Singapore.

Part I: Experiments

Materials: L-proline was purchased from Shanghai Kayon Biological Technology CO. Ltd. (Shanghai, China). Poly(vinyl pyrrolidone) (PVP, M_W=30,000), formaldehyde solution (HCHO, 40%), potassium tetrachloropalladite(II) (K_2PdCl_4) and copper chloride ($CuCl_2$) were purchased from Sinopharm Chemical Reagent Co. Ltd (Shanghai, China). Commercial Pd black was purchased from Johnson Matthey Corporation. All reagents were of analytical reagent grade.

Synthesis of concave CuPd@Pd tetrahedra: Typically, 58 mg of L-proline, 400 mg of PVP, 0.3 ml of K_2PdCl_4 solution (50 mM) and 0.1 ml of $CuCl_2$ solution (50 mM) were mixed with 6.5 mL of deionized water and stirred for 5 min. After adding 0.5 mL of HCHO into the homogeneous solution, the resulting homogeneous solution was transferred to a 20 mL Teflon-lined stainless-steel autoclave and heated at 140 ^oC for 4 h. After being cooled to room temperature, the obtained product was separated by centrifugation at 18000 rpm for 20 min, washed three times with deionized water and ethanol, and then dried at 60 ^oC for 5 h in a vacuum dryer.

Electrochemical measurements: All electrochemical tests were performed on a CHI 660D electrochemical analyzer (Shanghai, Chenghua Co.) at 30 ± 1 °C. A conventional three-electrode system was used, including a catalyst-modified glassy carbon electrode as a working electrode, a Pt wire as the auxiliary electrode, and a saturated calomel reference electrode (SCE). All potentials are reported versus the reversible hydrogen electrode (RHE), and for conversion of the obtained potential (vs. SCE) to RHE.

Prior to the electrode preparation, the samples were treated with Ultraviolet and visible (UV) irradiation (wavelength at 185 and 254 nm in air for 4 h) to remove the capping agent. For the preparation of the working electrode, an homogeneous suspension of catalyst was prepared by ultrasonic the mixture of 8 mg catalyst and 4 mL H_2O for 30 min, and 6 μL of the resulting

suspension was dropped on the surface of the glassy carbon electrode (3 mm diameter, 0.07 cm^2). After drying, 2 μL of Nafion solution (5 wt. %) was coated on the surface of the modified electrode and dried again. The total mass loading of the catalyst on the electrode was about 12 μg. Electrochemical measurements were performed in a 0.5 M N_2-saturated H_2SO_4 solution with or without 0.5 M HCOOH at a scan rate of 50 mV s^{-1}. Chronoamperometry curves were obtained in an N_2-saturated 0.5 M HCOOH + 0.5 M H_2SO_4 mixture solution for 3000 s at 0.1V.

Instruments: The morphology of the samples were determined by a JEOL JEM-2100F transmission electron microscopy operated at 200 kV, which is used to performing transmission electron microscopy (TEM), high-resolution TEM (HRTEM), selected area diffraction (SAED) and high-angle annular dark-field scanning TEM (HAADF-STEM). The samples were prepared through dropping the nanocrystal in ethanol dispersions onto carbon-coated Cu grids with a pipette and drying at room temperature. X-ray diffraction (XRD) patterns were recorded on a Model D/max-rC X-ray diffractometer using Cu Ka radiation source (λ =1.5406 Å) and operating at 40 kV and 100 mA. The composition of the catalysts was determined using the energy dispersive spectrum (EDS) technique. High-resolution X-ray photoelectron spectroscopy (XPS) was carried out on a Thermo VG Scientific ESCALAB 250 spectrometer with an Al Kα radiator, and the vacuum in the analysis chamber was maintained at about 10^{-9} mbar. The binding energy was calibrated by means of the C 1s peak energy of 284.6 eV. Ultraviolet and visible spectroscopy spectra were recorded at room temperature on a Shimadzu UV3600 spectrophotometer equipped with 1.0 cm quartz cells.

Part II: Figures and Tables

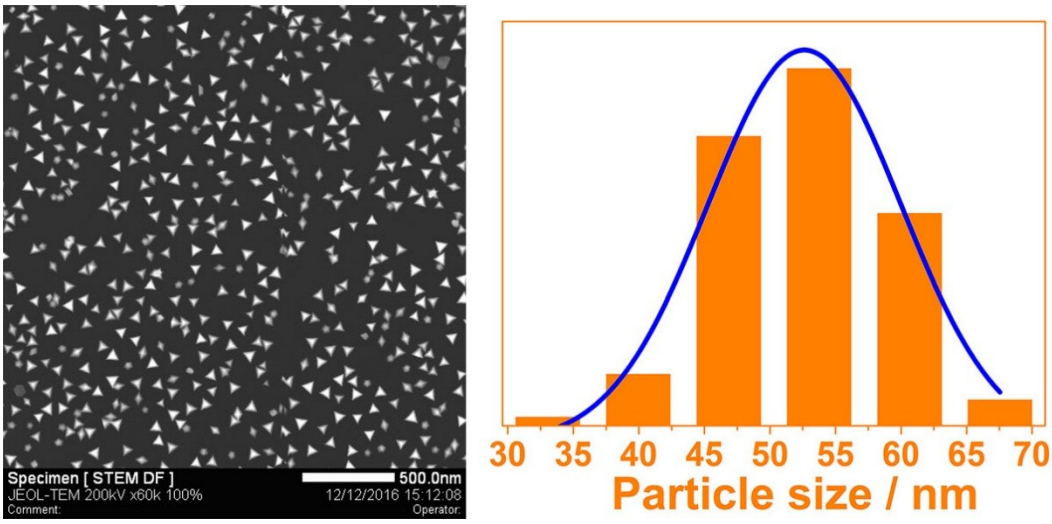

Fig. S1 STEM image and corresponding size histogram of concave CuPd@Pd tetrahedra.

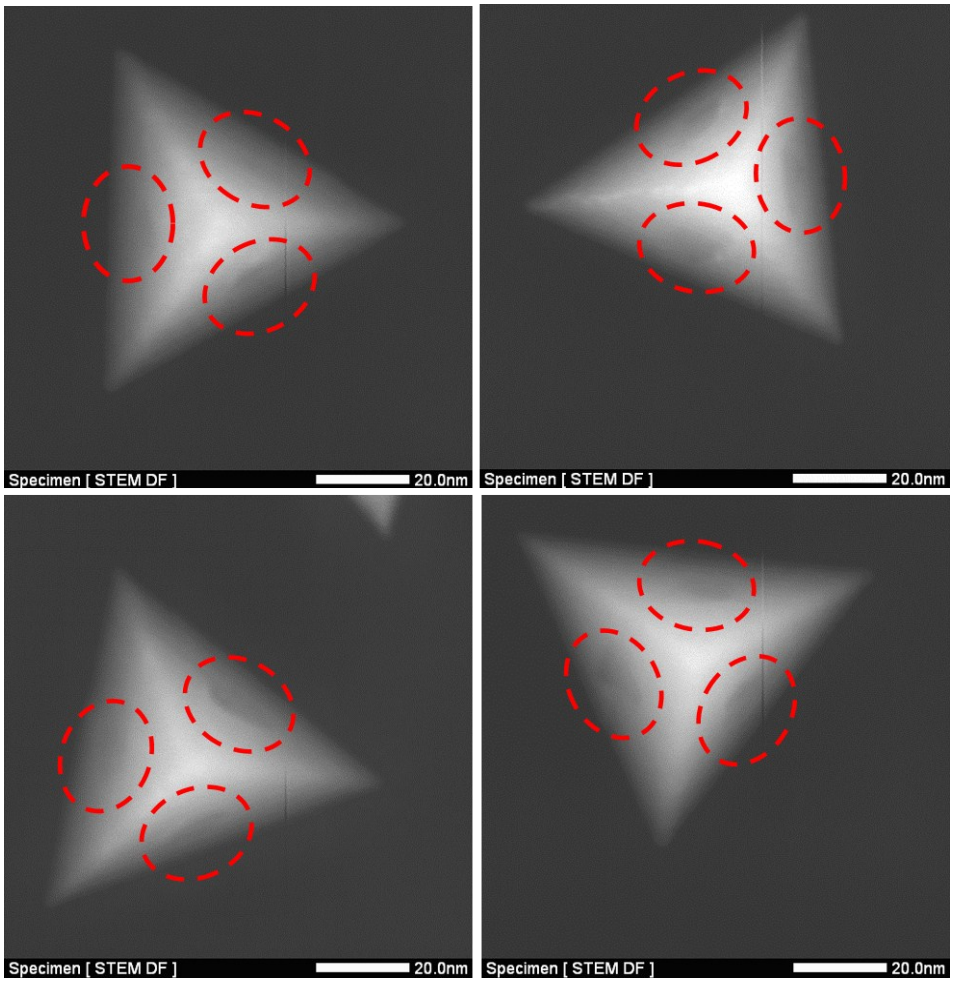

Fig. S2 STEM images of concave CuPd@Pd tetrahedra.

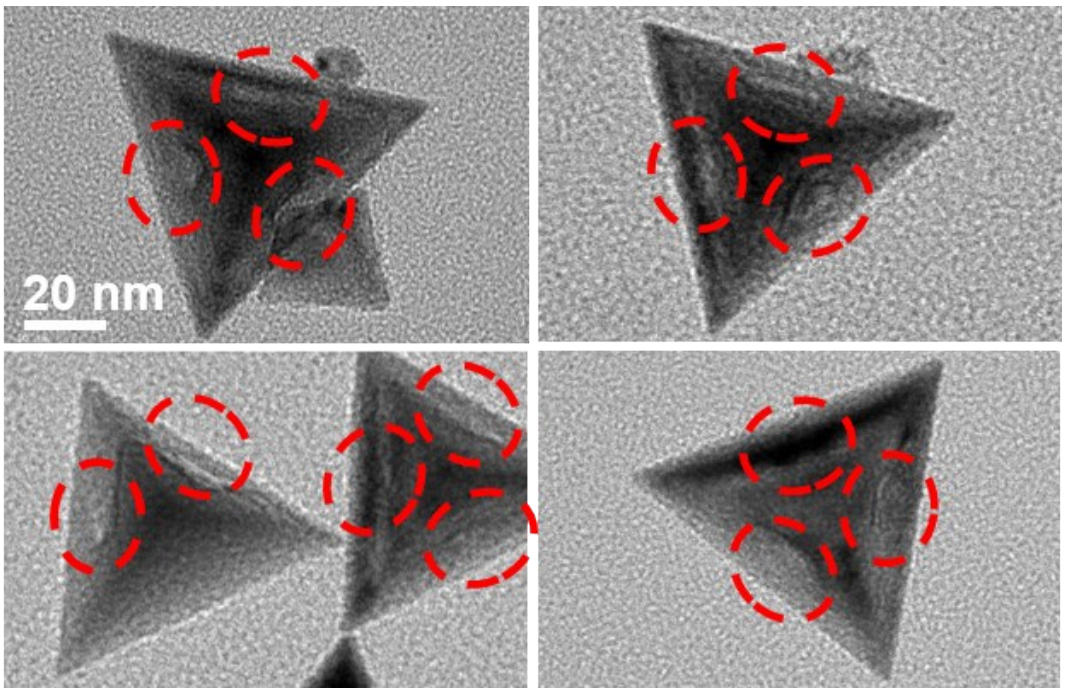

Fig. S3 TEM images of concave CuPd@Pd tetrahedra.

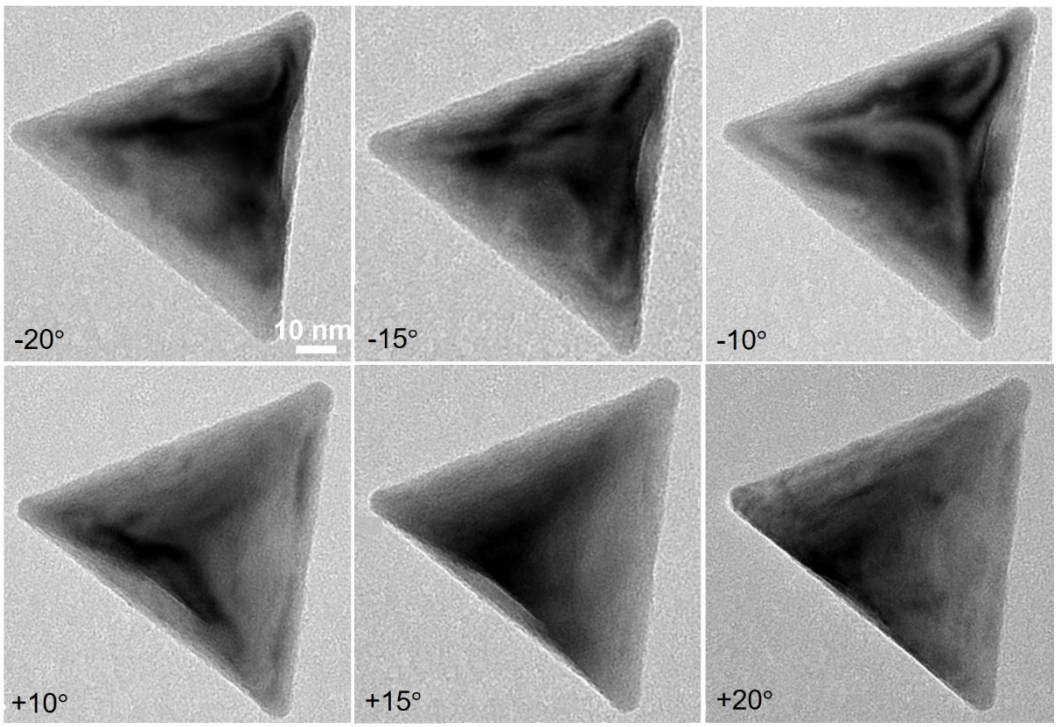

Fig. S4 Tilted TEM images recorded at different tilting angles of a single tetrahedron.

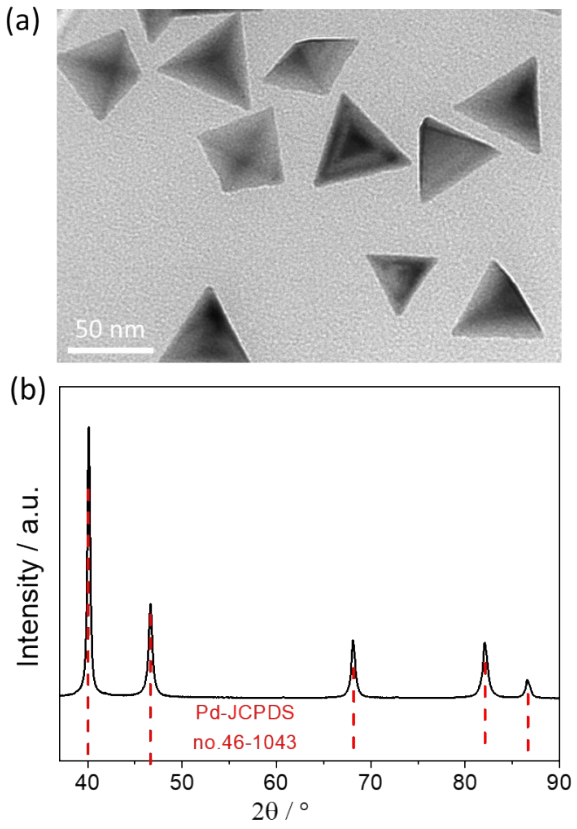

Fig. S5 (a) TEM images of Pd tetrahedra; (c) XRD pattern of Pd tetrahedra.

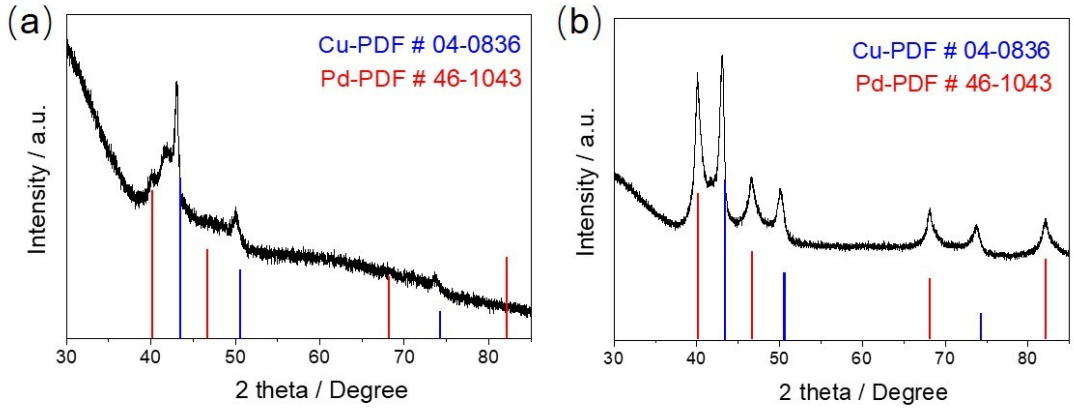

Fig. S6 XRD patterns of PdCu intermediates collected at (a)1 h and (b) 2 h.

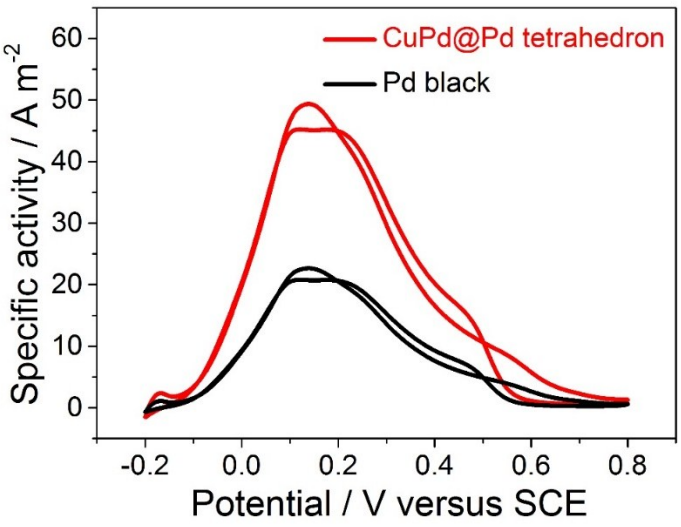

Fig. S7 Specific activity in 0.5 M H_2SO_4 + 0.5 M HCOOH solution at 50 mV s^{-1}.

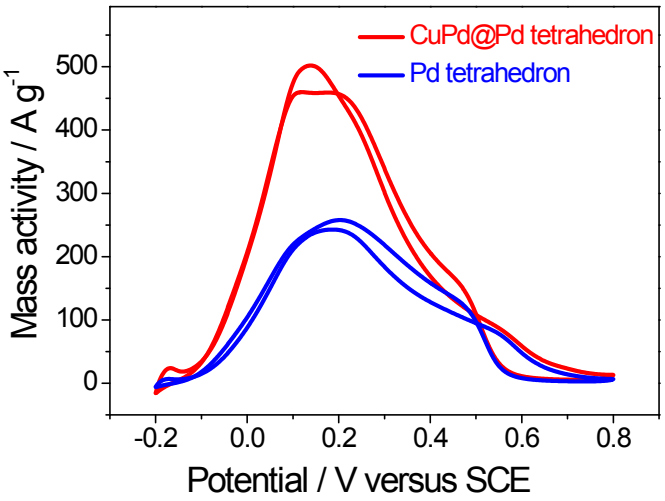

Fig. S8 CV curves of concave CuPd@Pd tetrahedra and Pd tetrahedra in N_2-saturated 0.5 M H_2SO_4 + 0.5 M HCOOH solution at 50 mV s^{-1}.

Table S1. Comparison of CuPd@Pd tetrahedra catalyst with the previous reported catalysts for the formic acid oxidation.

Catalyst	Mass activity ($mA\ mg^{-1}$)	Specific activity ($A\ m^{-2}$)	Electrolyte solution	Ref
PdCu@Pd	501.8	49.3	0.5 M H_2SO_4 + 0.5 M HCOOH	this work
Pd tetrahedra	259.2	39.6	0.5 M H_2SO_4 + 0.5 M HCOOH	this work
Pd black	200.7	20.8	0.5 M H_2SO_4 + 0.5 M HCOOH	this work
Pd_3Cu multipods	ca. 230	ca. 24	0.5 M H_2SO_4 + 0.5 M HCOOH	1
CuPd multipods	~	16.7	0.1 M $HClO_4$ + 1 M HCOOH	2
CuPd nanospheres	~	13.6	0.1 M $HClO_4$ + 1 M HCOOH	2
Pd-Cu-Fe/C	~	ca. 35	0.5 M H_2SO_4 + 0.5 M HCOOH	3
$Pd_{76}Cu_{24}$	120	ca. 8	0.5 M H_2SO_4 + 0.5 M HCOOH	4
Cu/Pd film	~	40	0.5 M H_2SO_4 + 1 M HCOOH	5
Porous $Pd_{75}Cu_{25}$	ca. 390	ca. 45	0.1 M $HClO_4$ + 1 M HCOOH	6
Porous PdCu	~	24.1	0.1 M $HClO_4$ + 0.2 M HCOOH	7
$Pd_{8.5}Cu_{1.5}$/C	353	~	0.1 M $HClO_4$ + 0.5 M HCOOH	8
PdCu/CNTs	267.97	~	0.5 M H_2SO_4 + 0.5 M HCOOH	9
Pd tetrahedron	~	30	0.5 M $HClO_4$ + 0.5 M HCOOH	10
Pd tetrahedron	237.6	~	0.1 M $HClO_4$ + 0.2 M HCOOH	11
Pd nanoconcave tetrahedron	459.6	~	0.1 M $HClO_4$ + 0.2 M HCOOH	11
Pd network	280.6	~	0.5 M H_2SO_4 + 0.5 M HCOOH	12
Pd nanodendrite assemblies	451.6	ca. 18	0.5 M H_2SO_4 + 0.5 M HCOOH	13
Pd dendrites	187.2	34.3	0.5 M H_2SO_4 + 0.5 M HCOOH	14
Pd nanosheets	409.3	~	0.5 M H_2SO_4 + 0.5 M HCOOH	15
Pd nanochain	309	~	0.5 M H_2SO_4 + 0.5 M HCOOH	15

Pd nanoflowers	211.3	~	0.5 M H_2SO_4 + 0.5 M HCOOH	[15]
PtAgCu@PtCu	314	~	0.5 M H_2SO_4 + 0.5 M HCOOH	[16]
PtCu nanoflowers	241	~	0.5 M H_2SO_4 + 0.5 M HCOOH	[16]
PdPt NP/CNT	197	~	0.5 M H_2SO_4 + 0.5 M HCOOH	[17]
E-TEK PdPt/C	100	~	0.5 M H_2SO_4 + 0.5 M HCOOH	[17]
Pd-Co assemblies	267	13.2	0.5 M H_2SO_4 + 0.5 M HCOOH	[18]
Porous PtAg@Pt	282.6	~	0.5 M H_2SO_4 + 0.5 M HCOOH	[19]

Part III: References

1. Y. Fan, Y. Zhang, H. Li, W. Shen, J. Wang and M. Wei, *RSC Adv.*, 2016, **6**, 43980-43984.
2. D. Chen, P. Sun, H. Liu and J. Yang, *J. Mater. Chem. A*, 2017, **5**, 4421-4429.
3. B. Yu, W. Wen, W. Li, Y. Yang, D. Hou and C. Liu, *Electrochimi. Acta*, 2016, **196**, 223-230.
4. F. Yang, Y. Zhang, P.-F. Liu, Y. Cui, X.-R. Ge and Q.-S. Jing, *Int. J. Hydrogen Energy*, 2016, **41**, 6773-6780.
5. R. Ojani, Z. Abkar, E. Hasheminejad and J.-B. Raoof, *Int. J. Hydrogen Energy*, 2014, **39**, 7788-7797.
6. C. Xu, Y. Liu, J. Wang, H. Geng and H. Qiu, *J. Power Sources*, 2012, **199**, 124-131.
7. A. Liu, H. Geng, C. Xu and H. Qiu, *Analyt. Chim. Acta*, 2011, **703**, 172-178.
8. P. Kyu-Hwan, L. Y. Wook, K. S. Wook and H. S. Woo, *Chem. Asian J.*, 2011, **6**, 1515-1519.
9. F. Zhu, G. Ma, Z. Bai, R. Hang, B. Tang, Z. Zhang and X. Wang, *J. Power Sources*, 2013, **242**, 610-620.
10. S.-I. Choi, J. A. Herron, J. Scaranto, H. Huang, Y. Wang, X. Xia, T. Lv, J. Park, H.-C. Peng, M. Mavrikakis and Y. Xia, *ChemCatChem*, 2015, **7**, 2077-2084.
11. Y. Zhang, M. Wang, E. Zhu, Y. Zheng, Y. Huang and X. Huang, *Nano Lett.*, 2015, **15**, 7519-7525.
12. Z. Guojie, Z. Lu, S. Liping, C. Yu, Z. Yiming, T. Yawen and L. Tianhong, *ChemPlusChem*, 2012, **77**, 936-940.
13. L. Zhang, Q. Sui, T. Tang, Y. Chen, Y. Zhou, Y. Tang and T. Lu, *Electrochem. Commun.*, 2013, **32**, 43-46.
14. J. Bai, L. Shen, D. Sun, Y. Tang and T. Lu, *CrystEngComm*, 2014, **16**, 10445-10450.
15. X. Qiu, H. Zhang, P. Wu, F. Zhang, S. Wei, D. Sun, L. Xu and Y. Tang, *Adv. Funct. Mater.*, 2017, **27**, 1603852.
16. G.-T. Fu, B.-Y. Xia, R.-G. Ma, Y. Chen, Y.-W. Tang and J.-M. Lee, *Nano Energy*, 2015, **12**, 824–832.
17. X. Li and I.-M. Hsing, *Electrochim. Acta*, 2006, **51**, 3477-3483.
18. L. Zhang, L. Wan, Y. Ma, Y. Chen, Y. Zhou, Y. Tang and T. Lu, *Appl. Catal. B: Environ.*, 2013, **138-139**, 229-235.
19. X. Jiang, X. Yan, W. Ren, Y. Jia, J. Chen, D. Sun, L. Xu and Y. Tang, *ACS Appl. Mater. interfaces*, 2016, **8**, 31076-31082.